BEC BIOENERGETICS COMMUNICATIONS
Bioenerg Commun 2022.8
https://doi.org/10.26124/bec:2022-0008
Open Access

Technical Communication

Cite
Baglivo E, Cardoso LHD, Cecatto C, Gnaiger E (2022) Statistical analysis of instrumental reproducibility as internal quality control in high-resolution respirometry. Bioenerg Commun 2022.8. https://doi.org/10.26124/bec:2022-0008

Author contributions
EB and EG analyzed the data and wrote the manuscript; LHDC and CC collected data; all authors approved the final version of the manuscript.

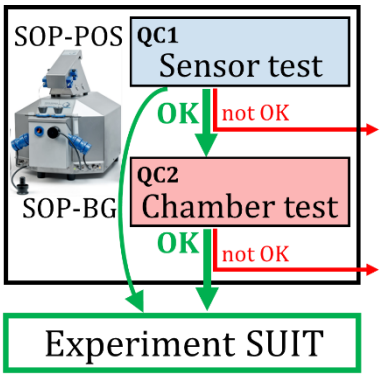

Conflicts of interest
EG is founder and CEO of Oroboros Instruments, Innsbruck, Austria.

Received 2022-05-09
Reviewed 2022-06-22
Revised 2022-07-11
Accepted 2022-08-01
Published 2022-08-04

Open peer review
Marcus Oliveira (editor)
Matheus Oliveira (reviewer)
Fernando Abdulkader (reviewer)
https://doi.org/10.26124/bec:2022-0008

Data availability
Zenodo
https://doi.org/10.26124/mitofit:2022-0018

Preprint
MitoFit Preprints 2022.18
https://doi.org/10.26124/mitofit:2022-0018.v2

Statistical analysis of instrumental reproducibility as internal quality control in high-resolution respirometry

Eleonora Baglivo, Luiza HD Cardoso, Cristiane Cecatto, Erich Gnaiger*

Oroboros Instruments, Innsbruck, Austria
* Corresponding author: erich.gnaiger@oroboros.at

Abstract

Evaluation of instrumental reproducibility is a primary component of quality control to quantify the precision and limit of detection of analytical procedures. A pre-analytical instrumental standard operating procedure (SOP) is implemented in high-resolution respirometry consisting of: (*1*) a daily SOP-POS for air calibration of the polarographic oxygen sensor (POS) in terms of oxygen concentration c_{O_2} [µM]. This is part of the *sensor test* to evaluate POS performance; (*2*) a monthly SOP-BG (background) starting with the SOP-POS followed by the *chamber test* quantifying the instrumental O_2 background flux. The chamber test focuses on the slope dc_{O_2}/dt [pmol·s^{-1}·mL^{-1}] to determine O_2 consumption by the POS and O_2 backdiffusion into the chamber as a function of c_{O_2} in the absence of sample. Finally, zero O_2 calibration completes the sensor test.

We applied this SOP in a 3-year study using 48 Oroboros O2k chambers. Stability of air and zero O_2 calibration signals was monitored throughout intervals of up to 8 months without sensor service. Maximum drift over 1 to 3 days was 0.06 pmol·s^{-1}·mL^{-1}, without persistence over time since drift was <0.004 pmol·s^{-1}·mL^{-1} for time intervals of one month, corresponding to a drift per day of 0.2 % of the signal at air saturation. Instrumental O_2 background $-dc_{O_2}/dt$ was stable within ±1 pmol·s^{-1}·mL^{-1} when measured at monthly intervals. These results confirm the instrumental limit of detection of volume-specific O_2 flux at ±1 pmol·s^{-1}·mL^{-1}. The instrumental SOP applied in the present study contributes to the generally applicable internal quality control management ensuring the unique reproducibility in high-resolution respirometry.

Keywords – high-resolution respirometry HRR; polarographic oxygen sensor POS; air calibration; instrumental background; reproducibility; limit of detection; internal quality control IQC; standard operating procedure SOP

1. Introduction

Quality control QC is essential to ensure experimental reproducibility. Proficiency testing PT aims at documenting and improving the technical performance of laboratories by independent quality assessments (Brookman, Mann 2021). PT targets the present lack of repeatability and reproducibility, and relies on implementation of PT schemes at substantial costs to accredited laboratories. Internal strategies may be implemented into laboratory science as practical steps towards PT to achieve reproducibility (Amaral, Neves 2021). In our study, we present an internal QC management tool (IQC) to evaluate the reproducibility of instrumental performance in high-resolution respirometry (HRR) using the Oroboros O2k (Oroboros Instruments, Innsbruck, Austria). We analyzed instrumental IQC tests performed in an experimental project conducted over three years (MiR05-Kit study). A follow-up report on these experiments is in preparation to analyze the reproducibility achieved with cultured cells as biological sample.

Instrumental testing represents IQC to assure the functioning of the instrument and to eliminate instrumental artifacts. In HRR the instrumental IQC tests — implemented as standard operating procedures (SOP) — are (*1*) daily oxygen *sensor tests* including air calibration in respiration medium, and (*2*) monthly *chamber tests* followed by zero calibration of the polarographic oxygen sensor (POS; Gnaiger 2001; 2008; Doerrier et al 2018). The stability of two-point calibrations (air and zero), and the response time and noise of the POS reflect the major performance characteristics of the sensor. The instrumental O_2 background flux (*BG*) in the absence of sample represents the chamber test to evaluate O_2 consumption independent of the sample and O_2 backdiffusion into the chamber as a function of O_2 concentration.

Diffusion of oxygen between an experimental chamber and its surroundings is zero in an ideal closed system. A closed system is defined in physical chemistry by system boundaries which prevent the exchange of matter — including oxygen — but allow for the exchange of energy, specifically exchange of heat under isothermal conditions in a thermostat. In reality, however, 'closed' experimental chambers may not perform as ideal closed systems. The aqueous phase (respiration medium) containing the sample within the chamber is separated by an oxygen-permeable membrane from the electrolyte, cathode, and anode of the POS. The electrochemical detection of c_{O2} in the respiration medium by the POS is based on O_2 consumption at the cathode, and as such, the experimental system is open for O_2 diffusion across the POS-membrane to the cathode. By design, the corresponding O_2 consumption by the POS is part of the instrumental O_2 *BG*. In contrast, any unwarranted leaks at the sealings of the closed chamber cause inappropriate O_2 backdiffusion into the chamber at declining experimental c_{O2}, resulting in artifacts of respirometric measurements, if not corrected for. The SOPs applied in the present study and the statistical analyses of instrumental tests provide the basis for evaluating the limit of detection and uncertainty in the measurement of volume-specific respiratory flux by HRR. Successful implementation of these IQC procedures into any experimental project on HRR and reporting of IQC results contribute to reproducibility and the quality of research in mitochondrial physiology.

2. Materials and methods

2.1. Chemicals

Mitochondrial respiration medium MiR05 (Gnaiger et al 2000): 0.5 mM EGTA, 3 mM $MgCl_2 \cdot 6H_2O$, 60 mM lactobionic acid, 20 mM taurine, 10 mM KH_2PO_4, 20 mM 2-[4-(2-hydroxyethyl)piperazin-1-yl]ethanesulfonic acid HEPES, 110 mM sucrose, 1 g/L BSA; pH 7.1 (KOH, 30 °C); prepared using MiR05-Kit (Oroboros Instruments, Austria, ID: 60101-01; MiPNet22.10 2022; Supplement S1) and BSA (bovine serum albumin, fraction V, Sigma-Aldrich, cat. N° A6003).

Chemicals for background test (MiPNet14.06 2020): Dithionite solution was prepared fresh using O_2-Zero Powder (Oroboros Instruments, ID: 26600-01): 0.017 g $Na_2S_2O_4$ was dissolved in 10 mL total volume phosphate buffer to obtain 10 mM dithionite solution. Phosphate buffer: 47 mM K_2HPO_4 (cat. N° P8281) and 3.3 mM KH_2PO_4 (cat. N° P5655) from Sigma-Aldrich. All solutions were prepared with deionized ultra-pure H_2O (Ultra ClearTMTP UV UF TM, Evoqua Water Technologies GmbH).

2.2. Open and closed chamber

2.1 to 2.5 mL MiR05 (pre-warmed to approximately 40 °C) were filled into the O2k-chamber containing the rotating stirrer. The stopper (calibrated for a chamber volume of 2 mL) was inserted completely, excess medium was siphoned off the stopper receptacle, and the stopper was partially pulled up into a position defined by the Stopper-Spacer (Oroboros Instruments, Austria; ID: 24420-01). This is defined as 'open chamber', in contrast to the 'closed chamber', referring to the condition of a fully inserted stopper with 2.0 mL aqueous medium and no gas phase in the chamber, 65 µL medium filling the stopper capillary, and excess medium siphoned off the stopper receptacle.

2.3. High-resolution respirometry

O_2 flux was measured in the Oroboros O2k. The O2k-chambers were calibrated at experimental volumes of 2 mL at experimental temperature of 37 °C (stability ±0.002 °C). The medium was continuously stirred with a polyether ether ketone (PEEK)-coated magnetic stirrer bar at 750 rpm. The O2k software DatLab 7.4 was used for data acquisition and analysis. The O_2 signal of POS was recorded at 2-s time intervals and volume-specific oxygen flux $J_{V,O2}$ [pmol·s^{-1}·mL^{-1}] was calculated real-time as the negative time derivative of O_2 concentration, $-dc_{O2}/dt$, and plotted continuously (Figures 1 and 2b).

A representative trace using the substrate-uncoupler-inhibitor-titration SUIT-001 protocol with HEK 293T cryopreserved cells (Doerrier et al 2018; Gnaiger 2020) illustrates the experimental protocol applied in a 3-year study on the stability of the MiR05-Kit (Figure 1). Experimental O_2 concentrations ranged from air saturation (180 µM) to a minimum of 30 µM in the entire study. To maintain this oxygen regime, several reoxygenations were required in the time course of experiments up to 2 h 30 min. Volume-specific O_2 flux $J_{V,O2}$ in various respiratory states is indicated in Figure 1, reaching a maximum of 140 pmol·s^{-1}·mL^{-1}. Antimycin A-inhibited residual oxygen consumption reached the limit of detection specified at 1 pmol·s^{-1}·mL^{-1} (MiPNet18.10 2019). The MiR05-Kit study included 8 O2k-Series H (16 chambers) in a one-day experiment (2019-12); 7 O2k-Series H (14 chambers) in a two-days experiment (3 days apart; 2020-11); and

8 O2k-Series I (16 chambers) in a two-days experiment (1 day apart; 2021-11). These instruments were used routinely in various other projects besides the MiR05-Kit study.

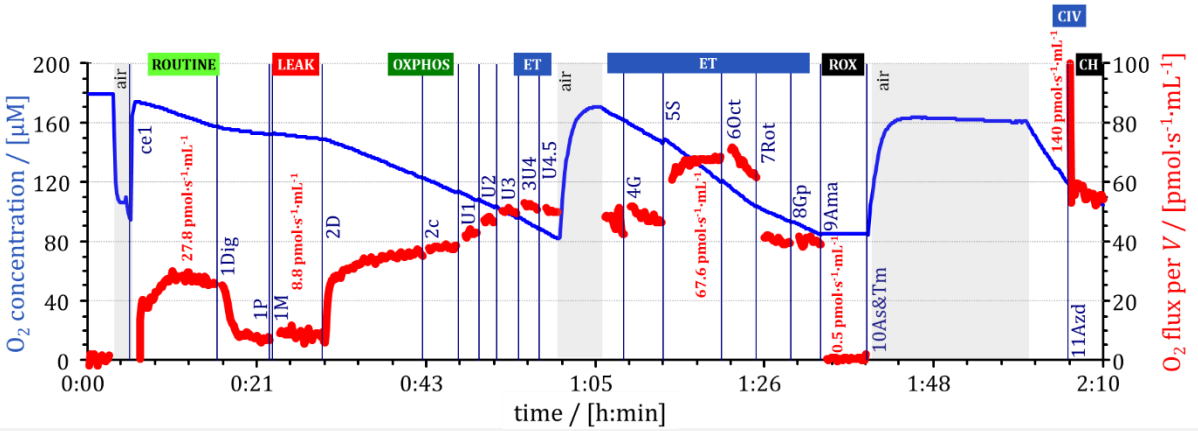

Figure 1. Experimental SUIT protocol. Trace of oxygen concentration (blue line) and volume-specific oxygen flux (red line; corrected for instrumental background O_2 flux *BG*) in the protocol SUIT-001 (Supplement S1) over a period of 2 h and 10 min. Oxygen concentration was kept above 80 µM by intermittent reoxygenations (open chamber, gray shade). Horizontal bars: respiratory states (selected corresponding rates are shown by numbers); vertical lines: events in sequential titrations. **ce1**: addition of HEK 293T cryopreserved cells (10^6 x·mL^{-1}) while the stirrer was stopped and the stopper intermittently removed, with subsequent ROUTINE respiration of living cells. **1Dig:** digitonin (10 µg·mL^{-1}) to permeabilize the plasma membrane. **1P** & **1M**: pyruvate (5 mM) & malate (2 mM), inducing LEAK respiration. **2D**: ADP (2.5 mM) to kinetically saturate OXPHOS capacity. **2c**: cytochrome *c* (10 µM) to test the integrity of the mitochondrial outer membrane. **U1** to **U4.5**: titrations of uncoupler (CCCP; numerals indicate the concentration [µM]), to obtain maximum oxygen flux (3U4) as a measure of electron transfer (ET) capacity; air: reoxygenation in the open chamber, when O_2 flux is not measured. **4G:** glutamate (10 mM). **5S**: succinate (50 mM). **6Oct**: octanoylcarnitine (0.5 mM). **7Rot:** rotenone (0.5 µM). **8Gp:** glycerophosphate (10 mM). **9Ama**: antimycin A (2.5 µM), inhibiting flux to residual oxygen consumption in state ROX. **10As&Tm**: ascorbate (2 mM) & TMPD (0.5 mM). After a 20 min period with an open chamber (air), As&Tm-stimulated CIV activity includes chemical autooxidation (CH) measured after inhibiting Complex IV by **11Azd:** azide (200 mM). Experiment 2021-11-16_P1-04 (data repository).

2.4. Settings of the TIP2k

The titration-injection micropump TIP2k (Oroboros Instruments; ID: 11100-03) is a standard module of the O2k. TIP2k syringes (200 µL) were filled with freshly prepared dithionite solution and mounted on the TIP2k. TIP2k-Filter papers (Oroboros Instruments; ID: 31320-01) were placed on the stoppers. TIP2k needles were inserted into the O2k-chambers through the stopper, avoiding contact with the stirrer bar in the chamber by adjusting the TIP2k-Needle Spacers. The TIP2k setup was loaded in the DatLab software and the TIP2k program was started for automatic control of dithionite injections at 20 min time intervals. After a delay of 20 min, the first dithionite injection was 0.25 µL/s, stopping at an O_2 concentration c_{O2} <100 µM. The second dithionite injection was 0.125 µL/s, stopping at c_{O2} <50 µM; the third injection at 0.05 µL/s stopped at c_{O2} <23 µM; finally, 50 µL dithionite was titrated in 1 s to reduce c_{O2} to 0 µM (SOP-BG, see Figure 2b).

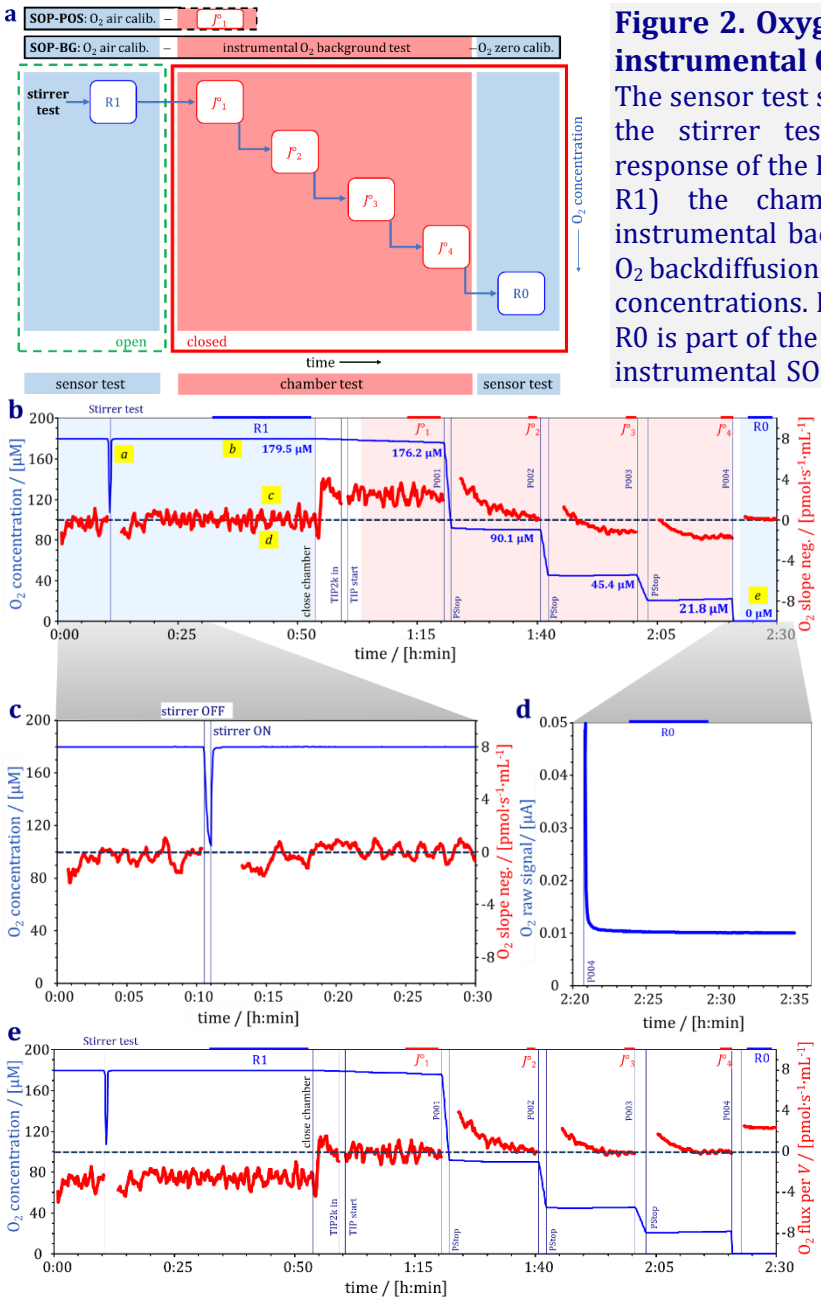

Figure 2. Oxygen sensor calibration and instrumental O_2 background test. The sensor test starts in an open chamber with the stirrer test, to evaluate the dynamic response of the POS. After air calibration (mark R1) the chamber is closed to measure instrumental background O_2 consumption and O_2 backdiffusion $J°_1$ to $J°_4$ at stepwise lowered O_2 concentrations. Finally, zero oxygen calibration R0 is part of the sensor test. **(a)** Scheme of O2k instrumental SOPs. SOP-POS: O_2 air calibration protocol, possibly continued by measurement of $J°_1$. SOP-BG: instrumental O_2 background protocol, combined sensor test and chamber test. **(b)** Representative traces of SOP-BG: Calibrated oxygen concentration (blue line [µM]) and negative slope (red line [pmol·s^{-1}·mL^{-1}]). Vertical lines represent events (P001 to P004: automatic TIP2k titrations), horizontal bars represent marks. Blue shaded sections indicate the sensor test. In the first section air calibration was performed in the open chamber including the stirrer test (panel c). When stability of the oxygen signal was reached (red line; zero slope), the air calibration signal R1 is obtained from the first mark set on the O_2 concentration plot. The final section of the sensor test represents zero oxygen calibration with mark R0 on the O_2 concentration plot (panel d), obtained in the closed chamber after titration of an excess concentration of dithionite which depletes O_2 completely. The red shaded section indicates the period of chamber test, when the chamber is closed and the TIP2k program started. During the first 20 min delay, O_2 consumption by the POS was recorded near air saturation (mark $J°_1$ on the red plot at 176.2 µM). The O_2 concentration was reduced stepwise to defined levels by the TIP2k program by injecting dithionite solution at 20 min time intervals. Marks $J°_2$, $J°_3$, and $J°_4$ were set at O_2 concentration of 90.1, 45.4, and 21.8 µM, respectively. The slope is not shown during the phases of dithionite-induced decline of O_2 concentration. Letters *a* to *e* refer to the discussion. **(c)** Zoom into the section of the stirrer test. Rotation of stirrers in both chambers was switched off for 30 s. After switching on the stirrer rotation, the increase of the oxygen signal should be rapid and mono-exponential. **(d)** Zoom into the oxygen signal at zero calibration R0, reached after complete reduction of O_2 in the closed chamber. **(e)** Trace of SOP-BG (panel b) after internal O_2 background correction. Sections are greyed during periods with open chamber and excess dithionite. Experiment 2021-05-06_P1-01_BG (QC data repository).

During titrations excess aqueous medium escapes the constant-volume chamber through the capillary of the stopper, maintaining a constant pressure. Liquid accumulating in the stopper receptacle equilibrates with room temperature and may cause convection at experimental temperature of 37 °C with corresponding transport of dissolved O_2 through the stopper capillary into the chamber. This is avoided by using TIP2k-Filter papers which soak up liquid in the stopper receptacle.

2.5. Oxygen sensor calibration and instrumental O_2 background test

The oxygen sensor test includes two calibration steps and quality control of (*1*) response time, (*2*) stability, and (*3*) noise of the sensor signal (Figure 2). Chambers were filled overnight or longer with 70 % ethanol, washed with H_2O, and filled with MiR05 (MiPNet19.03 2021). The sensor test was performed under experimental conditions in the absence of sample in an open chamber. First, the stirrer test was performed to evaluate the dynamic response of the POS. The stirring is switched off for 30 s. After switching on the stirrer rotation, a rapid and mono-exponential increase of the oxygen signal indicated a proper response time of the POS (Figure 2c). When MiR05 equilibrates with air in the gas phase, the oxygen signal reaches stability. Marks in DatLab define sections of a plot recorded over time. The air calibration mark R1 is set on the plot of the oxygen signal at air saturation. At an average barometric pressure of 94.9 kPa (Innsbruck; 575 m altitude), the partial O_2 pressure is 18.6 kPa, and equilibrium O_2 concentration in MiR05 is 180 µM (O_2 solubility 9.72 µM/kPa; MiPNet06.03 2022).

Next and still in the absence of sample, the chamber was closed by fully inserting the stopper – indicated by an event set in DatLab - to extrude the gas phase. This may cause a disturbance of the oxygen signal and a short fluctuation of the slope (Figure 2b). Subsequently, the needle of the TIP2k was inserted and the TIP2k program of DatLab started with a 20 min delay, during which O_2 consumption by the POS was recorded. Now the focus is switched from the sensor signal to the time derivative of O_2 concentration in the closed chamber, as the initial step of the chamber test. The mark $J°_1$ was set on the plot 'negative slope'. Subsequently the TIP2k program controls injections of dithionite solution at 20-min time intervals to reduce O_2 concentration to defined levels and allow for stabilization of the slope. Marks $J°_2$, $J°_3$, and $J°_4$ were set at the end of each interval when the slope was nearly constant, to calculate the median slope at the corresponding O_2 concentration for each mark. O_2 consumption by the POS is gradually compensated for by O_2 backdiffusion into the chamber at declining O_2 concentrations, eventually leading to a predominance of O_2 backdiffusion and a negative value of the negative slope.

At this point, the chamber test is concluded, and the focus is switched again to the oxygen signal. Sensor calibration is finalized by the TIP2k program, this time keeping the chamber closed (Figure 2a). An excess concentration of dithionite was titrated into the closed chamber, to completely reduce the oxygen, and the zero-oxygen calibration mark R0 is then set on the plot of the oxygen signal (Figure 2d).

Data was recorded at 2-s intervals. 60 data points were selected for the marks, but even 30 points were sufficient for obtaining reproducible results.

2.6. Sensor service

Service of the polarographic oxygen sensor (MiPNet19.18B 2021) was performed at intervals of a few months or more than one year to maintain high time resolution, low

noise, and signal stability of the sensor. This includes cleaning of cathode and anode, exchange of electrolyte, and membrane mounting. The sensor test helps to determine if a sensor service is required.

2.7. Statistics

The raw signal and slope of O_2 concentration in marked sections of the plots were computed by DatLab 7.4 as the medians of data points measured or calculated, respectively, within the marked sections.

In regressions between variables in X and Y with identical errors of measurement — see regressions between first and second calibrations (Figure 3c) — the ordinate Y/X slope b_Y is underestimated compared to the inverted X/Y slope b_X calculated from the abscissal X/Y slope β_X. The coefficient of determination r^2 is independent of inversion of the axes. At high r^2, mean inverted regression lines were calculated by inverted regression analysis using Excel (Gnaiger 2021). To minimize the residuals of both variables, Y and X, slopes b_Y and β_X and intercepts a_Y and α_X are calculated for the Y/X and X/Y inverted linear regressions, respectively. The mean slope $\bar{b} = (b_Y + b_X)/2$ and mean intercept $\bar{a} = (a_X + a_Y)/2$ are used, where $b_X = 1/\beta_X$ and $a_X = -\alpha_X/\beta_X$ (Gnaiger 2021). At r^2 close to zero, b_Y is nearly zero leading to a horizontal line, whereas b_X corresponds to a vertical line. In this case, mean slopes and intercepts are meaningless, and the inverted regression lines are shown separately to visualize the lack of a correlation. In regressions between $Y = -dc_{O2}/dt$ and $X = c_{O2}$, variability in X is small compared to variability in Y, hence ordinate regression analysis is appropriate (Figure 6).

3. Results

The limit of detection of $J_{V,O2}$ depends on accurate O_2 calibration of the POS, signal stability, and BG corrections of the slope over time as a function of O_2 concentration.

3.1. Oxygen calibration

A functional POS provides a sensitive and linear response to partial O_2 pressure with stable sensitivity. Sensitivity is the change of the raw signal [µA] divided by the change of O_2 concentration [µM] and averaged 0.011 µA/µM. Stability is evaluated either as a function of the deviation between the raw signals [µA] at two time points (from which the time-averaged drift can be calculated), or as a function of continuously measured drift [pmol·s^{-1}·mL^{-1}]. In addition, low noise and fast response of the oxygen signal to changes in O_2 concentration are required for adequate time resolution (Figure 2).

The instrumental O_2 background protocol SOP-BG was performed first for all sensors and chambers, followed by SOP-POS for the same sensors. The stability of calibration signals was evaluated over time intervals of 27 to 38 days in applications of SOP-BG (Figure 3a and b). When performing SOP-BG, the signal R0 is optionally calibrated as the final step. R0 ranged from 0.00 to 0.05 µA (Figure 3a; to 0.10 µA including the single maximum data point out of range). The maximal deviation between the two R0 calibration points - R0#1 and R0#2 - was 0.02 µA (0.08 µA including the maximum data point), indicating stability of R0 over a time interval of a month or longer. R0/(R1-R0) was maximally 2.2 % (5 % including the maximum data point), quantifying the magnitude of R0 on R1-R0 (Data repository QC_R1-R0). These results validate the monthly

performance of zero oxygen calibration. For the record, once a spurious R0 value (5.7 % of R1) was obtained in calibration R0#2 in O2k P7A in 2020. The calibration was repeated immediately without POS service, and the new R0#3 was accepted (1.5 % of R1) since it was consistent with calibration R0#1.

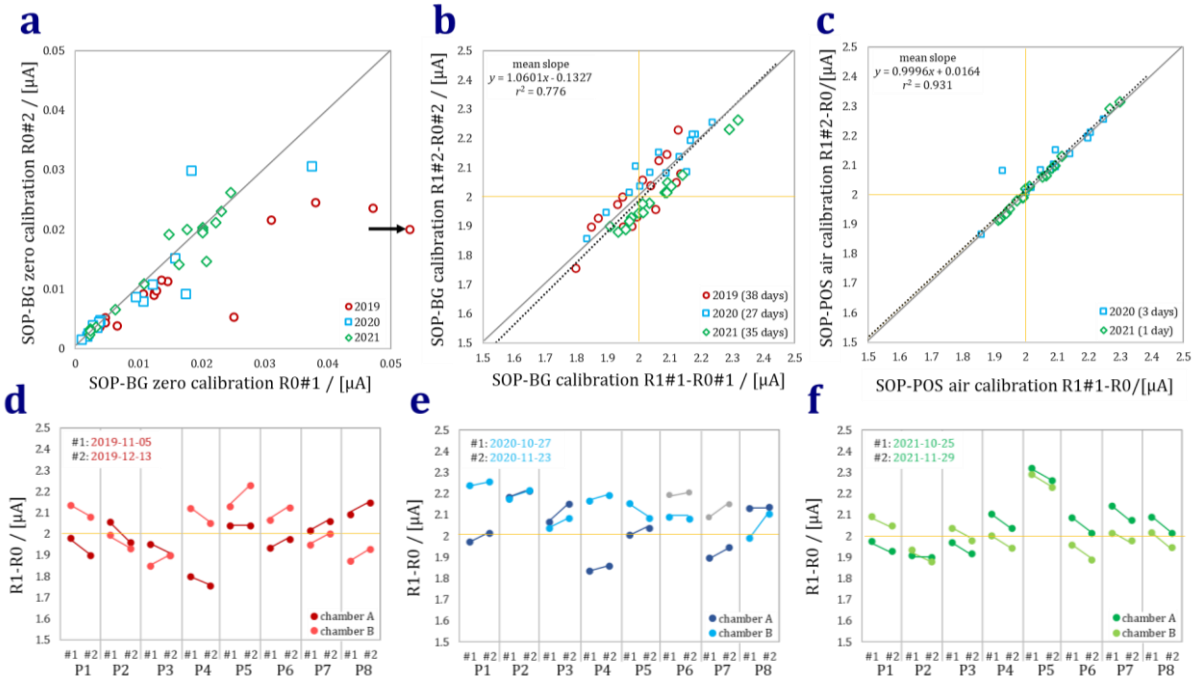

Figure 3. Stability of calibration signals of oxygen sensors over 1 to 3 days and 27 to 38 days. (a) Stability of zero oxygen calibration R0 of 46 POS measured in consecutive applications of SOP-BG (calibrations R0#1 and R0#2; 38, 27, and 35 days apart in 2019, 2020 and 2021, respectively). Arrow: single data point out of range at 0.10/0.02 (P5A in 2019). An especially good proportionality is shown in data from 2021 (r^2 = 0.93), while data from 2019 were more scattered (r^2 = 0.80). Full line: theoretical line of correspondence if calibrations #1 and #2 are identical. **(b)** Stability of R0-corrected air calibration signals of 46 sensors with R0 (panel a) and R1 measured in calibrations #1 and #2. Horizontal and vertical lines with intercept at 2/2: default R1 setting; full line: theoretical line of correspondence; dotted line: mean inverted regression line, indicating a proportional relationship (r^2 = 0.78). **(c)** R0-corrected air calibration signals R1-R0 [µA] of 30 POS with R1#1 measured in SOP-POS before each experiment (Figure 1) and R1#2 measured 3 or 1 days later (2020 and 2021, respectively). Horizontal and vertical lines with intercept at 2/2: default R1 setting; full line: theoretical line of correspondence; dotted line: mean inverted regression line, indicating a proportional relationship (r^2= 0.93). Experiments were restricted to a single day in 2019 and are, therefore, not applicable for this analysis. **(d)** to **(f)** R1-R0 signals, measured in SOP-BG (panel b), are shown for 16, 14, and 16 individual sensors (2019, 2020, and 2021, respectively). Chambers P6A and P7B were not used in the MiR05-Kit study in 2020. Dots with the same color and connected by lines represent values of calibrations #1 and #2 for the same sensor. Vertical lines separate different O2k.

Zero-corrected air calibration signals R1-R0 of 46 different POS ranged from 1.7 to 2.4 µA (Figures 3b). The variability is due to intrinsic differences between sensors and variation of membrane thickness when mounting and stretching the membrane on the sensor. The deviations between two calibration points are shown in Figures 3d to f. The

maximal deviations, divided by the number of days between measurements, corresponded to a time-averaged drift per day of 0.16 %, 0.21 %, and 0.10 % or 0.003, 0.004, and 0.002 pmol·s^{-1}·mL^{-1} for 2019, 2020 and 2021, respectively.

In contrast to R0, R1 calibrations were performed on these sensors not only in monthly time intervals but on each day before starting experiments with cells as biological sample. Applying the instrumental protocol SOP-POS (Figure 2a), the stability of the air calibration signal R1 of each sensor was evaluated over time intervals of 1 to 3 days (Figure 3c). As expected, stability of R1-R0 (using R0#1) values was improved when calibration R1#1 and R1#2 were separated by daily rather than monthly time intervals, demonstrating the advantages of daily R1 calibrations.

The deviation between daily calibrations R1#1 and R1#2 indicates a time-averaged drift per day of up to 1.0 % (or 2.7 % including the single data point with maximal deviation) for an O_2 concentration at air saturation of 180 µM. These values correspond to a slope of 0.02 nM·s^{-1}·or 0.02 pmol·s^{-1}·mL^{-1} (0.06 pmol·s^{-1}·mL^{-1} including the single data point). This low drift per day supports the standard R1 calibration procedure performed daily before the experiments (R1#1), without further consideration of the following R1#2. Comparing these values with the maximal slope of 0.004 pmol·s^{-1}·mL^{-1} calculated between calibrations separated by 27 to 38 days (Figure 3b), indicates that the maximal drift does not persist over the month.

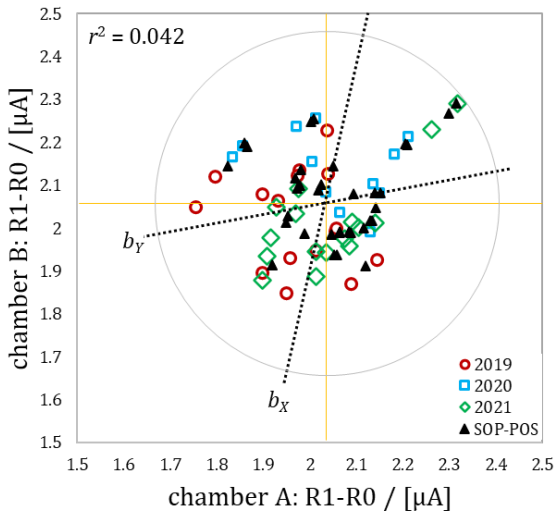

Figure 4. No correlation between calibration values in chambers A and B of the same O2k, measured simultaneously, indicating that each chamber can be considered independently in the experimental design. Dotted lines: ordinate b_Y and abscissal b_X regression lines, with a cross-over point of X^* = 2.03 µA and Y^* = 2.06 µA (vertical and horizontal lines), compared to the medians of 2.04 and 2.05 µA, close to the default value of 2 µA. Black symbols represent calibration signals with a time interval up to 3 days (SOP-POS). The circle, centered at the cross-over point, indicates the lack of interdependence with circular data distribution.

There was no correlation between the calibration values R1-R0 in chamber A and chamber B of the same O2k, measured simultaneously, confirming that each chamber can be considered independently in the experimental design (Figure 4).

Experiments in the MiR05-Kit study involving 40 POS were conducted within intervals of 3 to 8 months, during which air calibrations R1 were performed routinely in various O2k applications without sensor service and chamber disassembly. The relative change of R1 was generally <±0.10 over all time intervals (Figure 5; Data repository QC_Change of R1). R0 was maximally 1.8 % (2019 and 2020) and 1.9 % (2021) of R1, with a single value reaching 2.2 % (Data repository QC_R0 over R1).

The presented results point out the stability of oxygen calibration signals R1 and R0 for time intervals of (*1*) few days, (*2*) about one month, and (*3*) up to 8 months, and justify the applied SOP for air and zero calibrations (Supplement 2, Figure S2b).

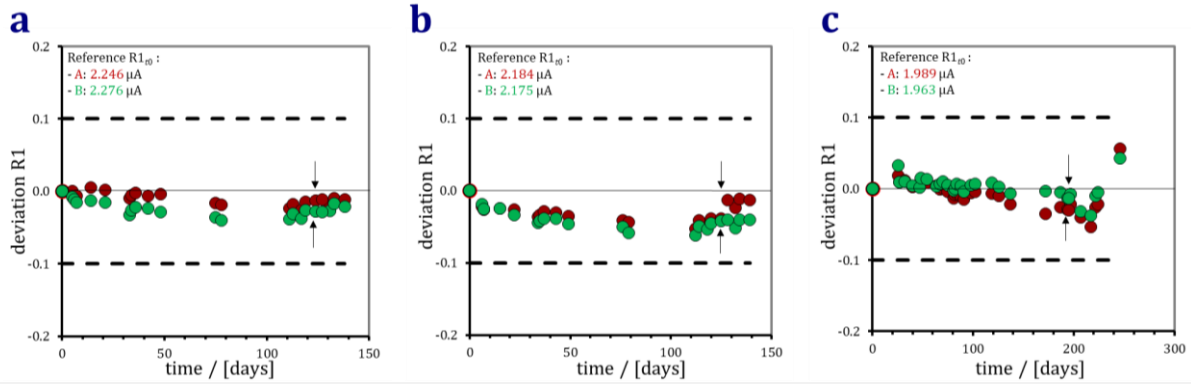

Figure 5. Stability of air calibration signals of oxygen sensors over time. Examples of 3 O2k at air saturation over 6 months (**a, b**; P2 and P3 in 2020) and 8 months (**c**; P2 in 2021). Red dots: chamber A; green dots: chamber B. The first R1 value after sensor service is shown as reference $R1_{t0}$ in each figure. The relative deviation of $R1_t$ over time is the fraction $(R1_t - R1_{t0})/R1_{t0}$. The relative change was generally less than ±0.10, indicating that R1 values were stable over time. The calibration points of the MiR05-Kit experiments (Figure 1) are indicated by arrows. All data: Data repository QC_Change of R1.

3.2. Instrumental O_2 background test

The O_2 background test (BG) is performed as a chamber test to (*1*) exclude any microbial contamination of the respiration medium, (*2*) quantify the O_2 consumption by the POS close to air saturation in mark $J°_1$ (O_2 concentration dropped from 180 to 176 µM), and (*3*) evaluate the deviation from an ideally closed chamber due to O_2 backdiffusion in sections marked as $J°_2$ to $J°_4$.

Linear regressions were calculated to express the dependence of the negative slope of the oxygen signal on O_2 concentration c_{O2}. For BG#1 the intercept $a°$ at zero c_{O2} ranged from -1.2 to -3.5 pmol·s^{-1}·mL^{-1} and the slope $b°$ from 0.021 and 0.035 in 40 different O2k chambers (Data repository QC_Background). Representative analyses are shown in Figure 6.

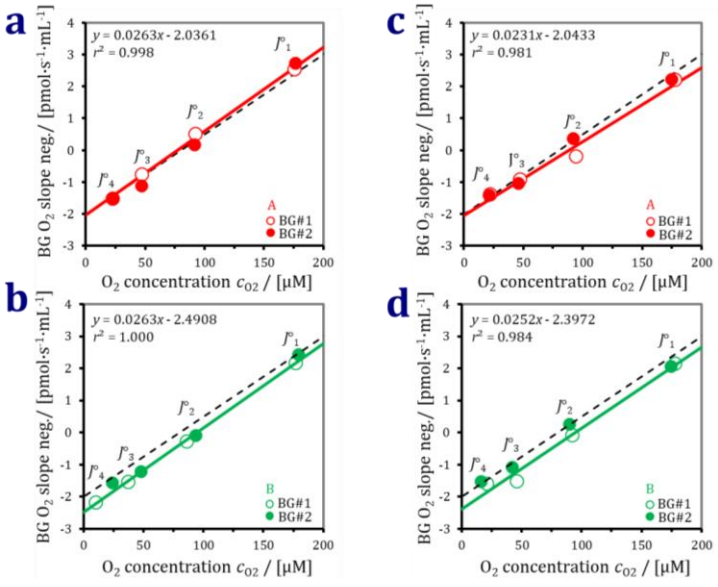

Figure 6. Stability of O_2 background test. Representative examples of 4 O2k chambers for background (BG) tests separated by 27 days (**a:** P8A, **b**: P8B; in 2020) and 35 days (**c:** P3A, **d**: P3B; in 2021). Negative BG O_2 slope plotted as a function of O_2 concentration for the four background marks ($J°_1$ to $J°_4$). Open circles: BG#1, with corresponding regression line (full line); closed circles: BG#2, showing the deviation from BG#1 regression line. Dashed lines: default intercept $a°$ = -2.0 pmol·s^{-1}·mL^{-1} and slope $b°$ = 0.025. $a°$ = 0 pmol·s^{-1}·mL^{-1} in an ideally closed chamber. All data: Data repository QC_Background.

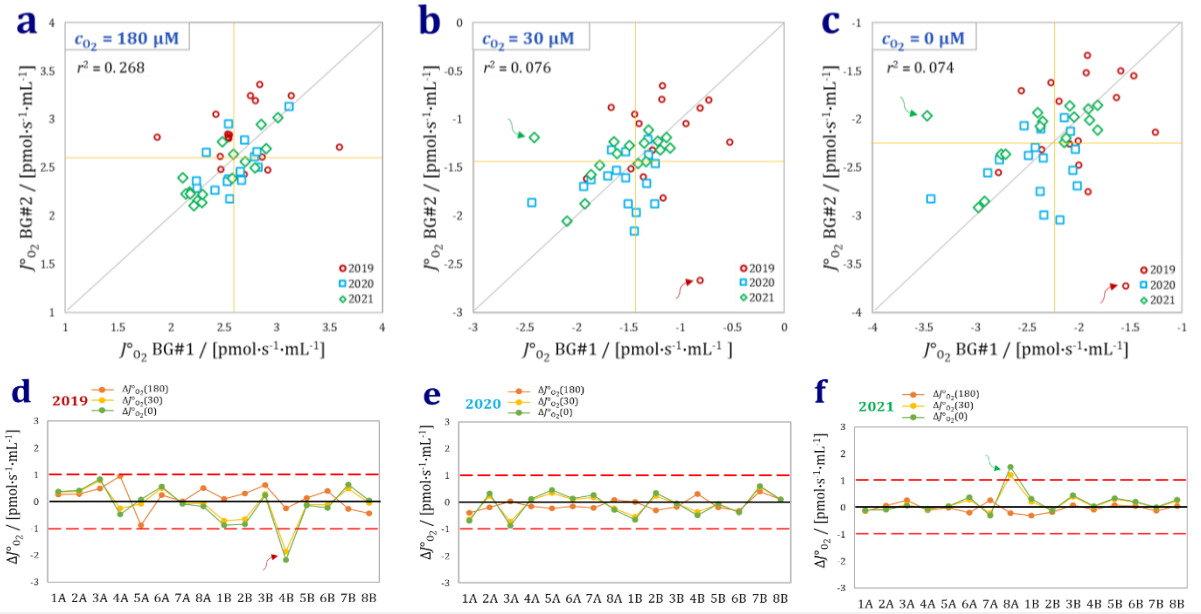

Figure 7. Stability of instrumental background O_2 flux at different O_2 concentrations up to 38 days. Instrumental background O_2 flux $J°_{O2}$ of 48 O2k chambers at O_2 concentrations 180 µM, 30 µM, and 0 µM in **(a), (b),** and **(c),** respectively. Full line: theoretical line of correspondence if $J°_{O2}$ of BG#1 and BG#2 are identical. Horizontal and vertical lines show the average intercepts of $J°_{O2}$ for each c_{O2}. Chamber 4B in 2019 indicated increased O_2 backdiffusion in BG#2 compared to BG#1 (red arrows). Chamber 8A in 2021 had higher O_2 backdiffusion in BG#1 compared to BG#2 (green arrows in panels b and c). **(d, e, f)** The difference $\Delta J°_{O2}$, evaluated as $J°_{O2}$(BG#2) - $J°_{O2}$(BG#1), of 48 O2k chambers at 180, 30, and 0 µM is shown for 2019, 2020, and 2021. $\Delta J°_{O2}$ values were evaluated for time intervals of 38, 27, and 35 days in 2019, 2020, and 2021, respectively. Dashed lines: limit of detection (±1 pmol·s^{-1}·mL^{-1}), indicating the residuals after background correction. 3 % of the data points exceeded the limit of detection for $\Delta J°_{O2}$(30) and $\Delta J°_{O2}$(0), in the same chambers identified by red and green arrows in panels b and c.

The stability of background corrections was evaluated for time intervals up to 38 days after BG#1, repeating the BG test in BG#2. Using the regression parameters, the instrumental background O_2 flux $J°_{O2}$ was calculated at air saturation (2.6 ± 0.3 SD pmol·s^{-1}·mL^{-1} at 180 µM), at the lowest c_{O2} observed in the MiR05 study (-1.4 ± 0.4 SD pmol·s^{-1}·mL^{-1} at 30 µM), and at the intercept for zero oxygen (-2.2 ± 0.5 SD pmol·s^{-1}·mL^{-1} at 0 µM; Figure 7).

The difference $\Delta J°_{O2}$ between $J°_{O2}$ of BG#2 and BG#1 at each c_{O2} was in the range ±1 pmol·s^{-1}·mL^{-1}, with two exceptions (chamber 4B from 2019 and 8A from 2021; Figure 7d to f). The absolute $\Delta J°_{O2}$ was maximally 0.9, 0.8 (or 1.9 with the data point out of range), and 0.9 (or 2.2 with the data point out of range) pmol·s^{-1}·mL^{-1} for 180, 30, and 0 µM, respectively. Use of the instruments besides the MiR05-Kit study varied for different O2k. A correlation between usage and background stability does not add information due to the small variation of $J°_{O2}$ between chambers in different instruments (Figure 7d to f).

In a similar analysis, we used BG#2 as an 'experimental mimetic' without sample to which the parameters of BG#1 were applied. The results are now expressed as respiratory flux per volume, which — in the absence of sample — should be zero. Deviations from zero directly express the error of background-corrected O_2 flux (Figure 8).

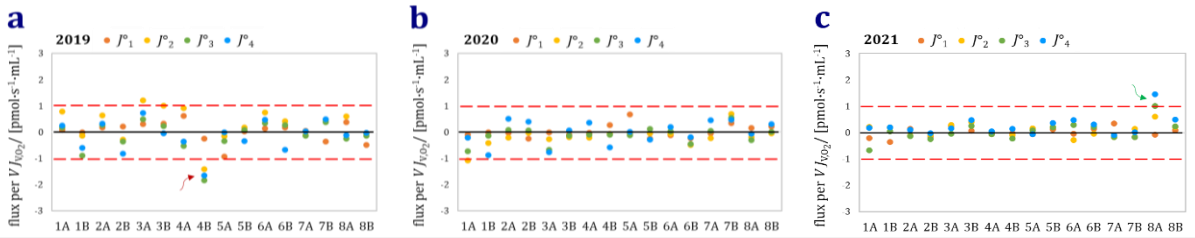

Figure 8. Application of instrumental BG#1 to BG#2 as an experimental mimetic. Data points shown in different colors represent the four background marks $J°_1$ to $J°_4$ (Figure 6), corresponding to O_2 concentrations of approximately 176, 92, 47, and 23 µM. Background-corrected respiratory flux per volume (BG#2) should be zero in the absence of sample. Compare Figure 7d, e and f.

In summary, these results suggest that the background correction performed with BG#1 was sufficient for a one-month period to obtain a limit of detection of $J_{V,O2}$ of ±1 pmol·s^{-1}·mL^{-1} in most cases, with only 3 % of the data extending to ±2 pmol·s^{-1}·mL^{-1}. The optimal time interval of performing SOP-BG may be modified based on individual experience and adjusted to the specific requirements for quality control in a particular project. Averaging BG#1 and BG#2 might improve the results further, but this option turned out to be unnecessary in most applications of high-resolution respirometry.

4. Discussion

Instrumental testing provides quality control to evaluate instrumental performance. The most comprehensive instrumental test in HRR is the SOP-BG (Figure 9). It includes both the sensor and chamber test and is obligatory before starting experiments with a newly assembled O2k. The SOP-BG, however, is time-consuming and therefore requires an economic planning of the frequency of conducting the entire procedure.

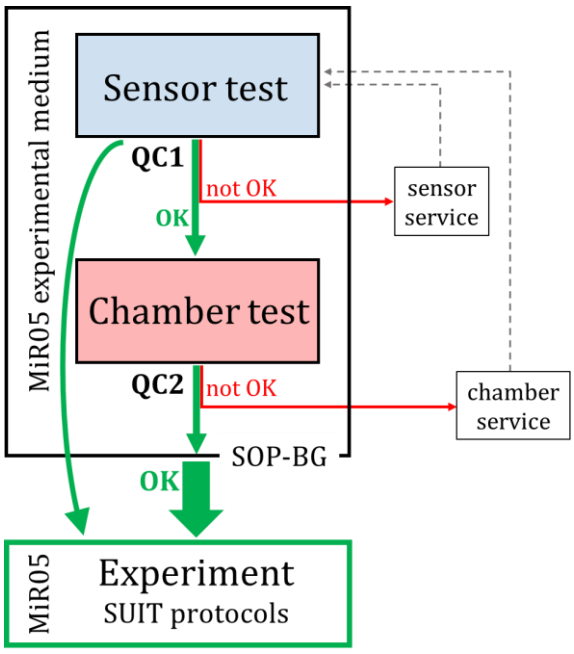

Figure 9. Quality control scheme for evaluation of instrumental performance by application of SOP-BG. QC1: sensor test, to check characteristics of the POS; if it fails, a sensor service is required. QC2: chamber test performed less frequently than QC1, to ensure the optimal functional state of the O2k chamber; if it fails, a chamber service is required. Statistical analysis of results in QC1 and QC2 provides the instrumental reference for interpreting the uncertainty of experimental results.

The sensor test represents the first quality control QC1, to check the functional characteristics of the POS and to decide on the necessity of performing a sensor service. The individual criteria of the sensor test are summarized in Figure 2b. (*a*) A rapid and mono-exponential response of the oxygen signal in the stirrer test (Figure 2c) is of primary importance in kinetic studies (Gnaiger 2001). The accurate response time is less important in analyses of respiratory states at constant

respiration, such as in SUIT protocols (Gnaiger 2020), except if the sensor response is as slow as to delay the effect of titrations on the respiratory rate. (*b*) The raw signal R1 was in a narrow range of 1.8 to 2.4 µA in different sensors. R1 was stable in every sensor over several months. (*c*) Signal stability was expressed as the time derivative $-dc_{O2}/dt$ within the section of R1 marks (medians). Stability was within ±1 pmol·s^{-1}·mL^{-1}, with a maximal absolute drift of 0.9 pmol·s^{-1}·mL^{-1} (Supplement 2, Figure S2a). (*d*) Noise of the signal was evaluated as the standard deviation (SD) of the data points in the plots of the O_2 slope. SD over a time interval of about 5 min was typically 0.6 pmol·s^{-1}·mL^{-1} (Figure 2b). Noise is related to the response time since a slower response acts effectively as a filter and implicates lower noise. (*e*) Zero calibration signals R0 were <2 % of R1, with a single value reaching 2.2 %.

Even if QC1 indicates a proper function of the oxygen sensor, the chamber test is required as QC2, since it reflects the characteristics of the respirometric chamber and the incubation medium. Any microbial contamination can be detected as an elevated instrumental background O_2 consumption $J°_1$ which is measured close to air saturation. This step is included in the daily SOP-POS and in the chamber test of SOP-BG followed by controlled variations of c_{O2} levels in the absence of sample. The range of c_{O2} selected in the chamber test should match the experimental oxygen regime (Pesta, Gnaiger 2012). At low oxygen levels, any leak of the chamber is detected as an increased O_2 backdiffusion. A proper outcome of both QC1 and QC2 minimizes instrumental errors and allows for evaluation of their effects on experimental results.

The limit of detection of O_2 flux is reported for HRR (Gnaiger 2001) but not for other respirometric instruments. Several comparisons of respirometric platforms provide narratives on the different experimental approaches without statistical evaluation of their performance relative to HRR (Horan et al 2012; Zhang et al 2012; Perry et al 2013; Schmidt et al 2021). In experiments using a multiwell platform, instrumental background data are not routinely reported (Seahorse XF Analyzer; Yépez et al 2018; Gnaiger 2021). To compare instrumental resolution in the XF Analyzer and Oroboros O2k, Zdrazilova et al (2022) evaluated background-corrected residual O_2 consumption measured in both platforms after inhibiting mitochondrial electron transfer by rotenone and antimycin A, obtaining minimum O_2 consumption used for baseline correction.

In the chamber test a linear regression expresses the dependence of the negative slope of the oxygen signal on c_{O2}. The regression parameters have default values in the DatLab software of $a°$ = -2.0 pmol·s^{-1}·mL^{-1} and $b°$ = 0.025, if no instrumental background test has been performed for calculating the experimental regression parameters. Using these default values, the instrumental background O_2 flux $J°_{O2}$ at air saturation (180 µM) and at 30 µM are calculated at 2.5 and -1.3 pmol·s^{-1}·mL^{-1} compared to 2.6 and -1.4 pmol·s^{-1}·mL^{-1}, respectively, obtained on average in our background tests (Figure 7). At this level of agreement, it may be asked why and how frequently a user of the O2k should perform the chamber test. Regular testing provides IQC, ensuring that (*1*) the instrument is in an optimally functional state, (*2*) the operators are shown to be skilled to follow properly the SOP, and therefore (*3*) instrumental artifacts are excluded. In summary, instrumental QC is a cornerstone for experimental reproducibility.

Further analysis of O_2 background parameters provides information on accuracy beyond reproducibility. Since O_2 diffusion is zero at air saturation, the instrumental background of 2.6 pmol·s^{-1}·mL^{-1} (Figure 7) is exclusively due to the O_2 consumption by the POS. The O_2 consumption by the POS, in turn, can be calculated from the electric

current. The current or calibration signal R1-R0 was 2.04 µA for the average sensor (Figure 3b). The flow of electrons of 1 A (= 1 C·s^{-1}) is converted to the molar format (chemical units) by the Faraday constant F = 96 485.33 C·mol^{-1}: the charge of 1 C is equal to the amount of 10.36 µmol of electrons e$^-$. Division by the charge number of 4 e$^-$/O_2 converts this amount of e$^-$ to 2.59 µmol of O_2 (Gnaiger 2020). Therefore, 2.04 µA corresponds to an O_2 consumption of 2.04 µC·s^{-1} · 2.59 µmol O_2 = 5.29 pmol O_2·s^{-1}, equal to a theoretical volume-specific background O_2 flux of 2.64 pmol·s^{-1}·mL^{-1} in a 2-mL chamber. Agreement between the O_2 flux calculated from the signal of the POS and the O_2 flux obtained experimentally confirms the accuracy of the measurement of O_2 consumption by HRR.

5. Conclusions

Quality control in HRR is essential to minimize experimental errors and ensure reproducibility. Instrumental tests are standard operating procedures that provide internal quality control for the evaluation of instrumental performance, to assure both the functioning of the instrument and correct execution of the SOP by the operator before starting an experimental series. The present study presents a generally applicable procedure which can be implemented into an external QC management and interlaboratory ring tests. These SOPs represent key aspects of proficiency testing, for improving technical performance of laboratories and development of certified auditing for diagnostic applications.

Abbreviations

BG	background
BG	instrumental O_2 BG flux
c_{O_2}	O_2 concentration
HRR	high-resolution respirometry
IQC	internal quality control
$J°_{O_2}$	instrumental background O_2 flux
J_{V,O_2}	volume-specific O_2 flux
POS	polarographic oxygen sensor
PT	proficiency testing
QC	quality control
R1-R0	zero-corrected air calibration signal
SD	standard deviation
SOP	standard operating procedure
SUIT	substrate-uncoupler-inhibitor titration

Acknowledgements

We thank Marco Di Marcello for technical support and performance of background experiments. This work was part of the Oroboros NextGen-O2k project, with funding from the European Union's Horizon 2020 research and innovation programme under grant agreement nº 859770.

References

Amaral OB, Neves K (2021) Reproducibility: expect less of the scientific paper. https://doi.org/10.1038/d41586-021-02486-7

Brookman B, Mann I, eds (2021) Eurachem guide: selection, use and interpretation of proficiency testing (PT) schemes (3rd ed). Available from www.eurachem.org

Doerrier C, Garcia-Souza LF, Krumschnabel G, Wohlfarter Y, Mészáros AT, Gnaiger E (2018) High-Resolution FluoRespirometry and OXPHOS protocols for human cells, permeabilized fibers from small biopsies of muscle, and isolated mitochondria. https://doi.org/10.1007/978-1-4939-7831-1_3

Gnaiger E (2001) Bioenergetics at low oxygen: dependence of respiration and phosphorylation on oxygen and adenosine diphosphate supply. https://doi.org/10.1016/S0034-5687(01)00307-3

Gnaiger E (2008) Polarographic oxygen sensors, the oxygraph and high-resolution respirometry to assess mitochondrial function. In: Mitochondrial dysfunction in drug-induced toxicity (Dykens JA, Will Y, eds) John Wiley & Sons, Inc, Hoboken, NJ:327-52.

Gnaiger E (2020) Mitochondrial pathways and respiratory control. An introduction to OXPHOS analysis. 5th ed. https://doi.org/10.26124/bec:2020-0002

Gnaiger E (2021) Bioenergetic cluster analysis – mitochondrial respiratory control in human fibroblasts. https://doi.org/10.26124/mitofit:2021-0008

Gnaiger E, Kuznetsov AV, Schneeberger S, Seiler R, Brandacher G, Steurer W, Margreiter R (2000) Mitochondria in the cold. In: Life in the Cold (Heldmaier G, Klingenspor M, eds) Springer, Berlin, Heidelberg:431-42. https://doi.org/10.1007/978-3-662-04162-8_45

Horan MP, Pichaud N, Ballard JWO (2012) Review: Quantifying mitochondrial dysfunction in complex diseases of aging. https://doi.org/10.1093/gerona/glr263

Perry CG, Kane DA, Lanza IR, Neufer PD (2013) Methods for assessing mitochondrial function in diabetes. https://doi.org/10.2337/db12-1219

Pesta D, Gnaiger E (2012) High-resolution respirometry. OXPHOS protocols for human cells and permeabilized fibers from small biopsies of human muscle. https://doi.org/10.1007/978-1-61779-382-0_3

Schmidt CA, Fisher-Wellman KH, Neufer PD (2021) From OCR and ECAR to energy: perspectives on the design and interpretation of bioenergetics studies. https://doi.org/10.1016/j.jbc.2021.101140

Yépez VA, Kremer LS, Iuso A, Gusic M, Kopajtich R, Koňaříková E, Nadel A, Wachutka L, Prokisch H, Gagneur J (2018) OCR-Stats: Robust estimation and statistical testing of mitochondrial respiration activities using Seahorse XF Analyzer. https://doi.org/10.1371/journal.pone.0199938

Zdrazilova L, Hansikova H, Gnaiger E (2022) Comparable respiratory activity in attached and suspended human fibroblasts. https://doi.org/10.1371/journal.pone.0264496

Zhang J, Nuebel E, Wisidagama DR, Setoguchi K, Hong JS, Van Horn CM, Imam SS, Vergnes L, Malone CS, Koehler CM, Teitell MA (2012) Measuring energy metabolism in cultured cells, including human pluripotent stem cells and differentiated cells. https://doi.org/10.1038/nprot.2012.048

Supplement S1. MiPNet and Bioblast links

MiPNet06.03 (2022) O2k Quality Control 1: Polarographic oxygen sensors and accuracy of calibration. Mitochondr Physiol Network 06.03(20):1-8.
- https://wiki.oroboros.at/index.php/MiPNet06.03_POS-calibration-SOP

MiPNet14.06 (2020) O2k Quality Control 2: Instrumental oxygen background correction and accuracy of oxygen flux. Mitochondr Physiol Network 14.6(08):1-16.
- https://wiki.oroboros.at/index.php/MiPNet14.06_Instrumental_O2_background

MiPNet18.10 (2019) O2k-specifications for respirometry and comprehensive OXPHOS analysis. Mitochondr Physiol Network 18.10(09):1-8.
- https://wiki.oroboros.at/index.php/MiPNet18.10_O2k-Specifications

MiPNet19.03 (2021) O2k-Chamber cleaning SOP and Integrated Suction System (ISS). Mitochondr Physiol Network 19.03(07):1-8.
- https://wiki.oroboros.at/index.php/MiPNet19.03_O2k-cleaning_and_ISS

MiPNet19.18B (2021) Service of the polarographic oxygen sensor OroboPOS. Mitochondr Physiol Network 19.18(B09):1-7.
- https://wiki.oroboros.at/index.php/MiPNet19.18B_POS-service

MiPNet22.10 (2022) Mitochondrial respiration medium: MiR05-Kit. Mitochondr Physiol Network 22.10(04):1-3.
- https://wiki.oroboros.at/index.php/MiPNet22.10_MiR05-Kit

SUIT-001 O2 ce-pce D003
- https://bioblast.at/index.php/SUIT-001_O2_ce-pce_D003 (retrieved 2022-07-07)

Supplement S2. Drift of the oxygen signal at air saturation

R1 is measured in the open chamber when the signal is expected to be constant at equilibrium with air. Maximal -dc_{O_2}/dt in mark R1 (Figure 2b; red plot) was 0.26 and 0.36 pmol·s^{-1}·mL^{-1}, while the minima were -0.39 and -0.86 pmol·s^{-1}·mL^{-1} in 2020 and 2021, respectively (Figure S2a). With a slight trend of increasing signals over time, the scatter indicated no persistence of drift of R1. Comparing these slopes in R1 with a maximum difference of 0.06 pmol·s^{-1}·mL^{-1} between R1#1 and R1#2 (Figure 3c) suggests that the apparent slopes in R1 were mainly due to short-term fluctuations of the oxygen signal.

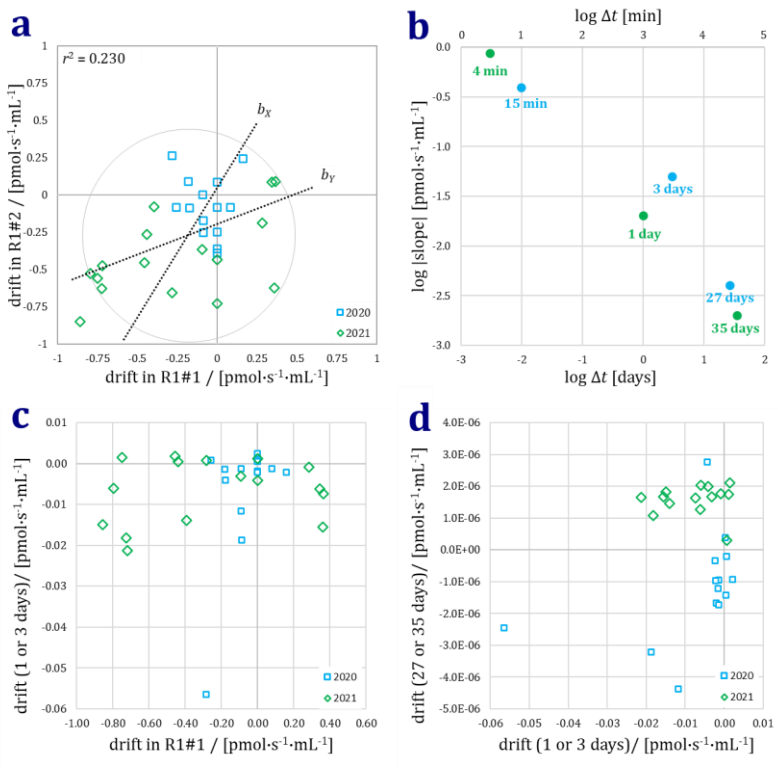

Figure S2. Signal drift for O_2 concentration over time at air saturation. (a) Drift estimated as negative c_{O_2} slope in marks R1 of 30 oxygen sensors measured in SOP-POS. R1#1 and R1#2 were 3 days (2020) or 1 day apart (2021). Horizontal and vertical lines: default intercept at 0/0. Dotted lines: ordinate b_Y and abscissal b_X regression lines, with cross-over points X^* = -0.17 pmol·s^{-1}·mL^{-1} and Y^*= -0.26 pmol·s^{-1}·mL^{-1}, compared to the medians of -0.09 and -0.25 pmol·s^{-1}·mL^{-1}. The circle, centered at the cross-over point, indicates circular data distribution with lack of correlation. Data points are within ±1 pmol·s^{-1}·mL^{-1}. **(b)** Maximal |dc_{O_2}/dt| (2020: blue dots; 2021: green dots) as a function of time intervals Δt from 4 minutes to 35 days on logarithmic scales. **(c)** and **(d)** Drift of 30 POS, evaluated as -(R1#2-R1#1)/[(R1#1-R0#1)/c_{O_2}*]/Δt, where c_{O_2}* is the O_2 concentration at air saturation in R1#1. Air calibrations #1 and #2 were 1 to 3 (SOP-POS) or 27 to 35 (SOP-BG) days apart. There was no relationship between drift evaluated over intervals of minutes and days (c) or days and a month (d).

The maximal absolute slope |dc_{O_2}/dt| for time intervals Δt of a few minutes (Figure S2a), few days (Figure 3c), and about one month (Figure 3b) decreased as Δt increased, averaging 0.6, 0.04 and 0.003 for a Δt of 4 to 15 min, 1 to 3 days and 27 to 35 days, respectively (Figure S2b). This suggests the lack of a persistent drift over time. The lack of correlation between short- and long-term drift indicates fluctuations of the oxygen signal, which do not affect the limit of detection of volume-specific flux (Figure S2c and d).